sciendo

POLISH MARITIME RESEARCH 4 (116) 2022 Vol. 29; pp. 105-114
10.2478/pomr-2022-0048

A CONVOLUTIONAL NEURAL NETWORK-BASED METHOD OF INVERTER FAULT DIAGNOSIS IN A SHIP'S DC ELECTRICAL SYSTEM

Guohua Yan
Yihuai Hu*
Qingguo Shi
Merchant Marine College, Shanghai Maritime University, China
* Corresponding author: *yhhu@shmtu.edu.cn (Y. Hu)*

ABSTRACT

Multi-energy hybrid ships are compatible with multiple forms of new energy, and have become one of the most important directions for future developments in this field. A propulsion inverter is an important component of a hybrid DC electrical system, and its reliability has great significance in terms of safe navigation of the ship. A fault diagnosis method based on one-dimensional convolutional neural network (CNN) is proposed that considers the mutual influence between an inverter fault and a limited ship power grid. A tiled voltage reduction method is used for one-to-one correspondence between the inverter output voltage and switching combinations, followed by a combination of a global average pooling layer and a fully connected layer to reduce the model overfitting problem. Finally, fault diagnosis is verified by a Softmax layer with good anti-interference performance and accuracy.

Keywords: Multi-energy hybrid ships, Inverters, Fault diagnosis, CNN

INTRODUCTION

Multi-energy hybrid ships can use both renewable sources of energy (wind, solar, etc.) and non-renewable energy (fossil fuels). In these ships, mechanical and electric propulsion is integrated through power coupling devices [1], which can not only save energy, reduce emissions, and meet the relevant requirements of International Maritime Organization (IMO), but also can effectively address the limitations of using a single energy supply. Hybrid power system ships initially used low-voltage DC distribution networks, and are gradually being developed to use medium- and high-voltage DC distribution networks. The application of variable speed shaft generator sets can significantly reduce fuel consumption and pollution emissions [2]. In this configuration, the variable speed diesel generator sets convert mechanical power into electrical energy, and the alternating current (AC) energy generated by each generator set is converted into direct current (DC) energy through rectifiers and pooled into a common DC bus. The energy storage devices are also connected to the same grid through bi-directional converters. The propulsion motors are then powered by inverters from the DC bus to drive the propellers forward and in reverse, to achieve motion of the ship. Compared with the traditional AC distribution network, this approach has advantages such as occupying less space and volume, faster and safer addition and removal of generator sets, simpler access to the system for energy storage devices, and better power quality [3]. With the development of hybrid

ships towards green energy, integration, and larger scales [4], power semiconductor devices are becoming widely used. These operate on pure electric propulsion, with variable propulsion motor power that is capable of reaching approximately 80% of the generator sets capacity [5]. The increasing power of the inverters used for electric propulsion of the ships makes them more likely to fail and to cause accidents, meaning that it is important to detect and diagnose these faults.

A six-switch, two-level, three-phase voltage source (2L-VSC) is a common topology for an electric propulsion inverter [6], and is a mature and reliable topology with a simple circuit structure and control strategy [7]. It mainly experiences short-circuit faults (SCFs) and open-circuit faults (OCFs) in the power switching transistors [8]. All faults in power electronic circuits are difficult to detect [9], and the inverter is one of the most vulnerable devices in a ship's DC distribution network [10]. Overloading, high temperatures, and incorrect drive signals can lead to SCFs, which occur within a very short time and are difficult to predict and diagnose. Research on the diagnosis of SCFs is scarce, and hardware protection is typically used [11], such as fast fuses for each transistor and inverters equipped with external current limiters to convert SCFs into OCFs. However, for high-power inverters, an approach based on fuse installation faces the problems of long protection times and an inability to protect the transistors from high transient electrical stress shocks [12], and the transistors may still be knocked out. Over-current limiters are the most effective and ideal methods of short-circuit protection for inverters, as they reduce the hazards generated by faults and limit the rate and capacity of a short-circuit current rise. They also makes it possible to detect, locate and isolate SCFs using algorithms [13], but suffer from problems such as voltage dips in fault situations. Hence, methods for the detection and diagnosis of OCFs in inverters are needed.

Fault diagnosis for inverters consists of two steps: the first is signal acquisition, in which sensors are used to obtain signals during operation, including the output voltage or current of the device, while the second is fault diagnosis and classification, in which suitable analysis and diagnosis methods are adopted to process the signals and to determine the condition of the device and the type and location of the fault. The inverter is usually allowed to continue working for a certain period under a power switching transistor OCF, and the propulsion motor can run for a short time, but the AC voltage and current output from the inverter is no longer balanced in this situation. If the inverter runs for a long time with the fault, the remaining power switching transistors will cause a secondary fault due to high current flow. Such faults should therefore be detected and located as soon as possible when they occur.

The ship's DC distribution network consists of numerous electrical and power electronic devices, which are coupled and interact with each other. This distribution network is complex, with many nonlinear factors, and it is difficult to use traditional fault diagnosis methods to detect and locate inverter faults in the network in a timely manner. Innovative diagnosis methods are therefore needed to achieve rapid diagnosis and location of inverter faults. Modern fault diagnosis methods are usually based on analytical models, and may be signal-based or data-driven [14]. Analytical model-based methods rely on the construction of accurate mathematical models, and diagnose faults by comparing the estimates of a model with the actual values. Signal-based methods are widely used for fault diagnosis; traditional techniques such as fast Fourier transform (FFT) [15] and variational modal decomposition (VMD) [16] are used to extract the features of faults, which are then generally used in conjunction with intelligent classification algorithms such as error backpropagation neural networks (BPNNs) and support vector machines (SVMs). A data-driven approach is more suitable for fault diagnosis of a ship's complex DC distribution network of inverters, but large amounts of historical data are required to establish a relationship between signals and faults. Many diagnostic methods have been proposed and applied to inverters [17-21]. Since traditional fault feature extraction methods such as FFT, principal component analysis (PCA), and VMD are linear (although classification methods such as BPNN and SVM have nonlinear capabilities), they have common defects, such as a tendency to fall into local minima [22] causing a loss of much useful information. The literature [23] contains a fault diagnosis method based on PCA and the multiclass relevance vector machine (mRVM). This approach uses PCA to downscale and extract the fault features for voltages and mRVM to locate the faults, which improves the efficiency and accuracy of inverter fault diagnosis. Compared with traditional feature extraction methods, deep learning (DL) methods with multiple nonlinear layers can mine more high-quality information from a large amount of data, and can significantly enhance fault diagnosis. In another study in the literature [19], an improved CNN-GAP model was used for fault diagnosis of inverters, and yielded an increased accuracy and reduced detection time compared to traditional CNN and SVM methods. Another study [22] combined an attention collaborative stacked long short-term memory (ASLSTM) network with a quantum particle swarm optimisation (QPSO) algorithm to intelligently tune the hyperparameters; this approach achieved fault diagnosis with multi-information feature fusion, and gave good results under constant loads, variable loads and noise. It can be observed that DL-based inverter fault diagnosis is generally better than traditional machine learning methods.

Deep autoencoders, deep belief networks, recurrent neural networks, and convolutional neural networks (CNNs) are the most widely used DL-based fault diagnosis models [24]. Of these, the CNN is one of the most important DL models, as it has very powerful feature extraction capabilities and has become a leading architecture. Although prior authors [25, 26] have used CNNs to diagnose inverter faults, the input to these networks was still determined by traditional feature extraction methods, meaning that the powerful feature extraction capability of the CNN was not exploited.

Current studies of inverter fault diagnosis are conducted based on the assumption of an ideal voltage source, but the ship's power grid has limited capacity, and its DC bus voltage

is constantly fluctuating within a small range. If the inverter of the propulsion motor fails, this will also have a strong impact on the ship's power grid. A one-dimensional CNN-based diagnosis method is proposed in this paper to automatically locate the fault using the waveform of the output voltage, based on the interaction between the inverter fault and ship's limited-capacity grid. From an analysis of the principle of operation of the inverter, its three-phase output voltage is selected as the input data for the fault diagnosis. For the one-to-one correspondence between inverter output voltage and the combined switch, the output voltage is simplified. A combination of a global average pooling (GAP) layer and a fully connected (FC) layer is used to reduce overfitting and computation.

DC ELECTRICAL SYSTEMS OF SHIPS

MULTI-ENERGY HYBRID SYSTEMS

In a parallel hybrid ship, mechanical and electric propulsion are integrated, and the two propulsion systems can operate independently or in coupled mode [1]. When the main engine power is sufficient, the electric motor connected to it via the power coupling device can also work in power generation mode, and can supply power to the main grid through the rectifier. The propulsion mode can be selected based on the ship's operating conditions, giving a highly flexible system that can maximise the efficient use of energy and reduce emissions.

We consider a 7382 tonnes multi energy hybrid bulk carrier with a parallel hybrid electrical power system, as shown in Fig. 1. This multi-energy hybrid ship has four modes of operation:

(1) Host propulsion mode (direct push mode): The power coupling device is only connected to the host, and the propeller is driven to rotate by two hosts.

(2) Individual motor operation mode (PTH mode): The shaft belt motor works in motor mode, the power coupling device is connected only to the motor, and the propeller is driven to rotate by two motors.

(3) Simultaneous propulsion mode (PTI) for the main engine and shaft belt motor: The shaft belt motor works in motor mode and is connected only to the main engine through a power coupling device to jointly drive the propeller rotation, and the generator set supplies power to the shaft belt motor and the whole ship load.

(4) Host-driven propeller and shaft with generator mode (PTO mode): The main machine is in working mode, and the axle belt motor is in generator mode, absorbing energy from the main machine through the power coupling device for power generation and transmitting power to the main DC grid through the rectifier.

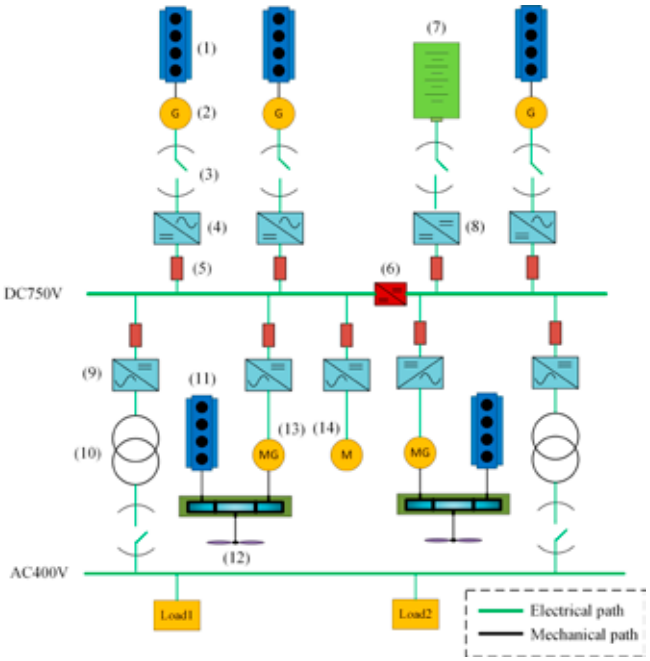

(1) LNG-fueled diesel engines (2) Asynchronous generators (3) Grid-connected switch (4) AC/DC (5) Fast fuse (6) Solid state circuit breakers (7) Li-ion battery pack (8) Bidirectional DC/DC (9) DC/AC (10) Isolation transformer (11) Diesel engine (12) Propeller (13) Propulsion motor/alternator (14) Bow side thrust

Fig.1. Configuration diagram for the power system of a 7382 tonnes multi-energy hybrid bulk carrier

Tab/ 1. Main parameters for a 7382 tonnesmulti-energy hybrid bulk carrier

Ship type	Bulk carrier	Ship size	114.8 × 17.50 × 8.30 m
Main parameters of generators	AC 400 V 50 Hz 350 kW	Main parameters of Propulsion motor	AC 400 V 50 Hz 1000 RPM 500 kW
AC/DC power	400 kW	Diesel engine	648 kW
Li-ion battery capacity	161k Wh	DC/AC power	600 kW

The 2L-VSC inverter contains six fully controllable devices (IGBTs) and six uncontrollable devices (power diodes), and its topology is shown in Fig. 2. The six switching tubes in the inverter circuit are set sequentially at 60° intervals, with a conduction angle of 180°, and three switching tubes are on simultaneously at any given moment. To avoid two switching tubes on the same bridge arm conducting at the same time and causing an SCF, a very short time interval needs to be added between the instants at which the previous switch turns off and the next switch turns on.

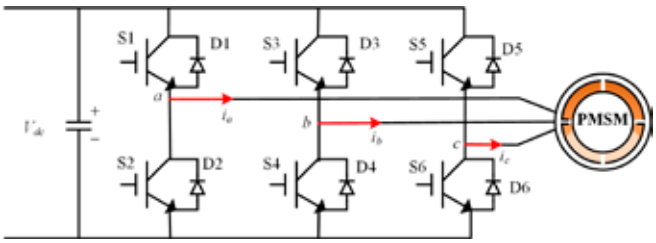

Fig. 2. Topology of a two-level three-phase voltage source inverter

It can be seen from the topology in Fig. 2 that the 2L-VSC inverter consists of three groups of six switches, and the upper and lower switches of the same bridge arm must be in opposite states, meaning that there are eight switch combinations for the three groups of switches. To simplify the description, the power switch tube is set to one to represent an open state and zero for a closed state. The correspondence between the condition of each inverter switch and the three-phase output voltage can then be obtained as shown in Table 2.

Tab. 2. Relationships between inverter switching states and three-phase output voltages

Item	S_1	S_2	S_3	S_4	S_5	S_6	u_{an}/V_{dc}	u_{bn}/V_{dc}	u_{cn}/V_{dc}
0	0	1	0	1	0	1	0	0	0
1	0	1	0	1	1	0	−1/3	−1/3	2/3
2	0	1	1	0	0	1	−1/3	2/3	−1/3
3	0	0	0	0	1	0	−2/3	1/3	1/3
4	1	0	0	1	0	1	2/3	−1/3	−1/3
5	1	0	0	1	1	0	1/3	−2/3	1/3
6	1	0	1	0	0	1	1/3	1/3	−2/3
7	1	0	1	0	0	0	0	0	0

From Table 2, we see that the switch states 1–6 represent the operating state of the inverter, and the output voltage to the external load is non-zero. When the switch is in state 0 or state 7, the inverter output voltage is zero. Assuming that the power switch is an ideal device and ignoring the effect of dead bands, the inverter output voltage under normal conditions can be derived as follows:

$$\begin{cases} u_{an} = [S_1(S_4 + S_6) - S_2(S_3 + S_5)]V_{dc}/3 \\ u_{bn} = [S_3(S_2 + S_6) - S_4(S_1 + S_5)]V_{dc}/3 \\ u_{cn} = [S_5(S_2 + S_4) - S_6(S_1 + S_3)]V_{dc}/3 \end{cases} \quad (1)$$

SIGNAL ANALYSIS OF INVERTER SIGNALS

Since the inverter can operate for a short time under an OCF, it is still common to install a fast fuse in the hardware circuitry to handle an inverter SCF by converting it into an OCF. As can be seen from Eq. (1), the inverter has a unique corresponding output voltage under any switch combination. If one of the power switch tubes fails, the output voltage waveform will be obviously different from the normal state; the output voltage waveforms also differ with different failed power switch tube. The probability of several power switching tubes failing at the same time in an inverter is very low, and we therefore consider only the cases of a single OCF and a dual OCF in this paper. The topology of the 2L-VSC inverter indicates that there are six types of faults when a single-tube OCF occurs, and 15 types of faults when a double-tube OCF occurs. Faults can be divided into several types according to the location of the fault and its impact on the phase voltage, as shown in Table 3.

Tab. 3. Fault settings for the two-level three-phase voltage source inverter

Inverter status	Fault type	Faulty power switching tubes	Fault number
Normal	None	None	Normal
Single tube fault	Single tube fault	S_1	S_1
		S_2	S_2
		S_3	S_3
		S_4	S_4
		S_5	S_5
		S_6	S_6
Dual tube fault	Single-phase power loss fault	S_1, S_2	S_1S_2
		S_3, S_4	S_3S_4
		S_5, S_6	S_5S_6
	Fault with different phase, same side	S_1, S_3	S_1S_3
		S_1, S_5	S_1S_5
		S_3, S_5	S_3S_5
		S_2, S_4	S_2S_4
		S_2, S_6	S_2S_6
		S_4, S_6	S_4S_6
	Fault with different phase, different side	S_1, S_4	S_1S_4
		S_1, S_6	S_1S_6
		S_2, S_3	S_2S_3
		S_3, S_6	S_3S_6
		S_2, S_5	S_2S_5
		S_4, S_5	S_4S_5

The type of signal has a strong impact on the diagnosis of a inverter fault. Although studies in the literature [27, 28] have used the inverter output current as a fault diagnosis signal, the operating conditions of the propulsion motor are variable and complex, which can have a great impact on the current and can easily cause misdiagnosis. Some authors [23, 29] have used the inverter output voltage as the analysis object, which is less affected by load variation than current and has more significant fault characteristics, and their results have also shown good diagnostic ability. However, all of these works involved analytical studies of individual inverters or of the closely connected rear stages, and were carried out under stable, interference-free conditions of the supply grid. In reality, for multi-energy hybrid ships, the grid capacity is very limited, and the capacity of the propulsion

motor can sometimes reach more than 80% of the capacity of the generator set; this means that the failure of an inverter will inevitably have a strong impact on the grid, and the fluctuation of the grid will in turn affect the output voltage of the inverter to a large extent. In this paper, we consider a multi-energy hybrid power system in which the three-phase output voltage from the inverter is selected as the input data for fault diagnosis, as this can reflect the situation after inverter failure more realistically. Fig. 3 shows the waveforms for the DC bus voltage and output voltage under normal, single-tube and double-tube faults of the inverter when the system is stable.

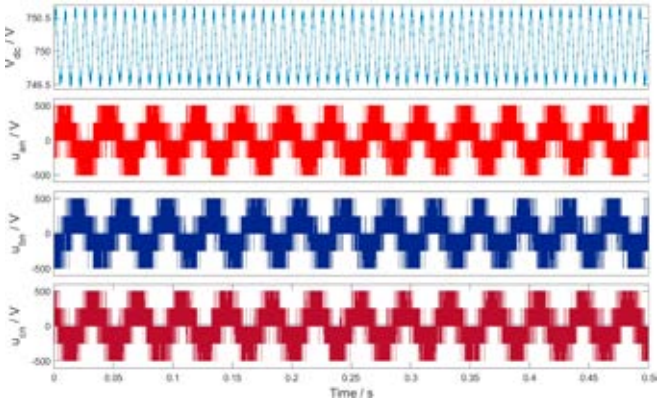

(a) DC bus voltage and inverter phase voltages in no-fault conditions

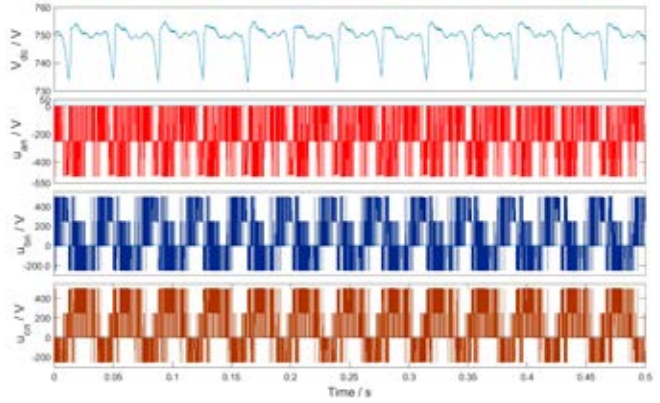

(b) DC bus voltage and inverterphase voltages for S_1 single-tube-faul

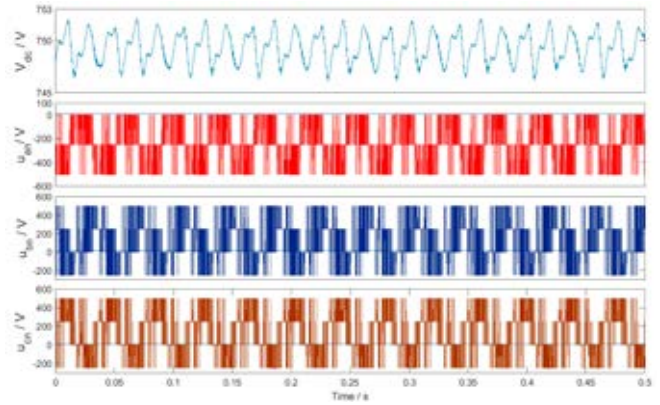

(c) DC bus voltage and inverter phase voltages forS_1,S_2 dual-tube-faul

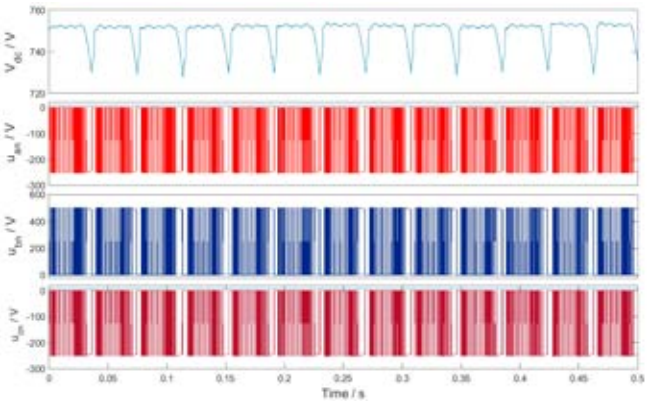

(d) DC bus voltage and inverter phase voltages for S_1,S_5 dual-tube-faul

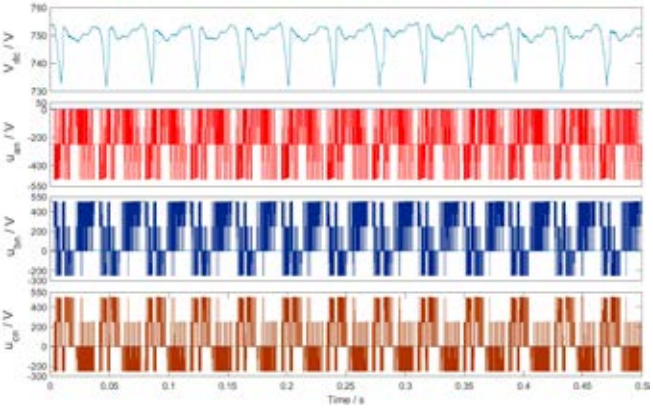

(e) DC bus voltage and inverter phase voltages forS_1,S_6 dual-tube-faul

Fig.3. DC bus voltage and output voltage waveforms for different states of the inverter

As can seen from Fig. 3, the output voltage waveforms of the inverters under different conditions are not the same in any voltage cycle, which provides a basis for fault diagnosis from the voltage signal. The fluctuation in the bus voltage under an inverter fault is much larger than that under normal conditions, and this is caused by an unbalanced three-phase current due to the fault. The controller generates a drive signal based on the set speed and sends it to the inverter. If there is an OCF, the power switch tube that should be conducting cannot pass the current, and no current will pass through the phase where the motor is connected to this switch tube. The controller controls the remainder of the fault-free phases to pass the maximum current in advance, to allow the motor to reach the set speed. Due to the large capacity of the propulsion motor, a short period of high current will go through, the impact on the grid will be large and the generator set will undergo hysteresis, meaning that it will be too late to react, with a sudden drop in bus voltage. The lithium battery set will automatically be accessed when the bus voltage is below 740V, in order to supply additional power to the grid to stabilise the bus voltage.

FAULT DIAGNOSIS USING A ONE-DIMENSIONAL CNN

From the analysis in the previous section, it can be seen that the output voltage of the inverter under any switch combination has unique, significant fault characteristics, regardless of whether or not the power switch tube is faulty. Hence, the three-phase phase voltage output from the inverter is selected as input to the CNN in our study. Multi-energy hybrid ships typically operate in PTH mode under no-load conditions. In this mode, the electric propulsion unit is responsible for the navigation of the ship and the inverter works close to its full load, meaning that it is most prone to failure. In this paper, we therefore simulate the output three-phase voltage of the single-side inverter under 22 different conditions, including single-tube and dual-tube faults, and a dataset is bulitfrom a multi-energy hybrid power system model in Matlab/Simulink for the PTH mode. These faults are simulated by artificially zero drive signal of power switching tubes for 48 s for each type. The rated speed of the propulsion motor is 1000 rev/min, and the minimum stable running speed is 200 rev/min. From motor speed regulation theory, it is known that the higher the motor speed, the shorter the inverter output voltage cycle. Hence, in order to ensure that each group of sample data contains at least one complete voltage cycle, we simulate various working conditions at 200 rev/min, and the sampling time for each group of samples is 0.1 s. This gives a total of 4000 x 3=12,000 sampling points for each group of samples, and a 480 groups of sample data are obtained for each type. Of these, 240 groups are used for training of the CNN model, 90 for validation, and 150 for testing.

DATA PRE-PROCESSING

The three-phase phase voltages output from the inverter have the form of two-dimensional data with consistently high dimensionality, meaning that they are difficult to process and classify with a one-dimensional CNN. From Eq. (1), we see that there is also a specific relationship between the three phase voltages output from the inverter at the same moment, regardless of whether the inverter is faulty or not, and this relationship is determined by the controllable switching combination. To address this feature, a data processing method is proposed in which the three-phase voltage data at the same sampling point are arranged according to u_{an}, u_{bn}, and u_{cn} while the timing is still in the form of the original sampling order. The three phase voltages are rearranged in such a way as to reduce the data from two dimensions to one dimension, while retaining the information in the original data. Fig. 4 shows the details of the downscaling process, where u_{ann}, u_{bnn}, and u_{cnn} are the three-phase voltages at the sampling points t_n, n = 1, 2, 3, respectively. The three-phase phase voltage output by the inverter is less affected by the change in load, which directly reflects the operating state of the inverter and is more effective when used for inverter fault diagnosis than the current signal. The three-phase phase voltage is the phase voltage between the inverter and the propulsion motor, and additional voltage-measuring equipment is required in the transmission line to obtain these signals.

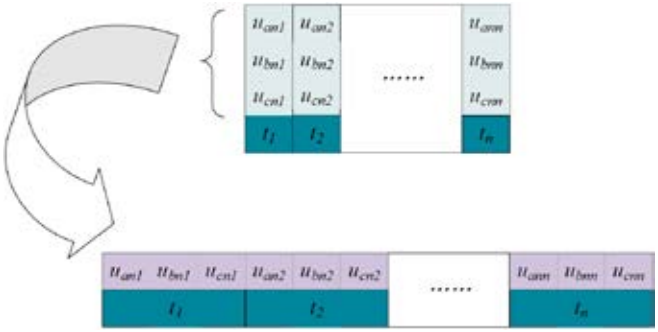

Fig. 4. Degradation process of the three-phase phase voltage

CNN NETWORK

The current trend in CNN models is to use increasing numbers of network layers and smaller convolutional kernels, as small convolutional kernels can obtain better local information while deeper networks can obtain better global information.

A deep CNN structure was therefore designed as shown in Fig. 5. The input layer handled the processed voltage data (batch size: 12,000, 1), and the network extracted the features with three convolutional layers. The convolutional kernels of the three convolutional layers were all of 3×1 size , as small convolutional kernels have fewer parameters. The number of convolutional kernels in the first convolutionallayer was 16, and the convolutional step was three. Because the voltage data were dimensionally reduced in the form of original data the three points data were filed to completely characterise the state of the inverter.

The number of convolutional kernels increases with the depth of the network, due to the reduced computation volume of the previous network after pooling, which can be provided computational ability to the additional convolutional kernels. Since an increase in the number of layers makes the extracted features more abstract, an increase in the number of convolutional kernels is a better way to combine the previously learned features of the network, as it provides more comprehensive coverage of various features. Although the FC layer can obtain all the features extracted from the convolutional layer, there is a parameter explosion and redundant parameters, and the network is prone to overfitting. Adding an FC layer can improve overfitting but makes the network more bulky. A combination of GAP layer and FC layer is therefore carried out. The GAP layer can integrate high-dimensional information output from the convolutional layer, which directly achieves a significant reduction in the number of feature parameters. The layer has no parameters, meaning that overfitting can be avoided and the network has better robustness. The final classification layer is a commonly used Softmax layer, which is used to output

the probability of each fault. The ReLU activation function is used between the first convolutional layer and the final classification layer, and each convolutional layer contains layer normalisation (LN) operations, as shown in Fig. 5. The main parameters of the network are listed in Table 4.

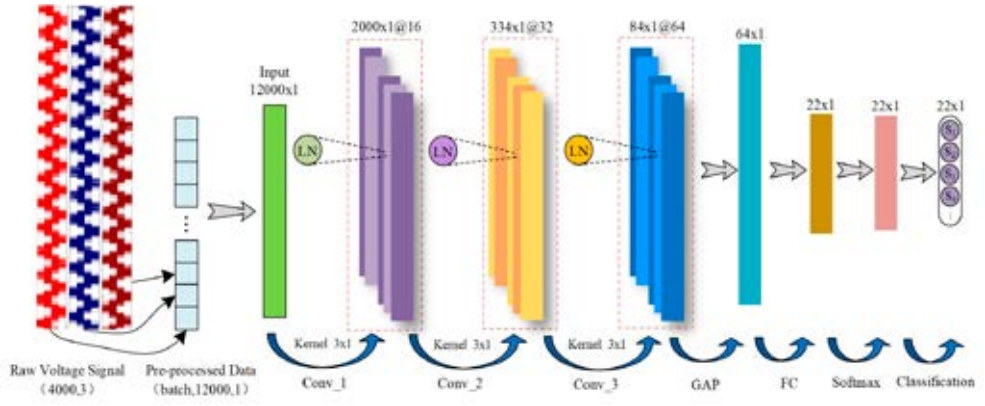

Fig. 5. Structure of the CNN with the global average pooling method

Tab. 4. Main parameters of the CNN network

Layer	Size	Number	Step length	Output size	No. of parameters
Input				12000×1	0
Conv_1	3×1	16	3	4000×1×16	160
Average pooling	2×1		1	2000×1×16	0
LN1		16			32
Conv_2	3×1	32	1	667×1×32	1568
Average pooling	2×1		1	334×1×32	0
LN2		32			64
Conv_3	3×1	64	1	167×1×64	6208
Average pooling	3×1		1	84×1×64	0
LN3		64			128
GAP	84×1	64	84	64×1	0
FC				22×1	1430
Softmax	22	1		22	0

HYPERPARAMETERS OF THE CNN

The hyperparameters of CNN models have an important impact on the training process and the model representation. There is no mature theory to guide the setting of hyperparameters, and a trial and error method is usually used; the results are then combined based on experience and the outcome of training, in a continuous effort to obtain appropriate hyperparameters, which requires a large number of training iterations. An optimiser is a tool that can guide the neural network to update the parameters using an optimisation algorithm, which can effectively improve the training speed of the model and allow it to find the optimal solution quickly. Stochastic gradient descent with momentum(SGDM) improves the problem of traditional SGD oscillation, and also helps the network to jump out of local minima and to find better network parameters when the network tends to converge in the middle and late stages of training and the network parameters oscillate back and forth around local minima.

In this study, a segmented constant decay learning rate was chosen for parameter updating, with a large learning rate to allow the network to converge quickly to find the optimal solution. The learning rate was then gradually reduced to ensure the stability of the model in the later training period. The initial learning rate was 0.01, and this was reduced by half after every 10 epochs. Other measures were also taken to reduce the overfitting problem, such as rearranging data at the end of each iteration, and the main parameters of the optimisation algorithm were set as shown in Table 5.

Tab. 5. Main parameters of the optimisation algorithm

Optimisation algorithm	SGDM	Shuffle	Every epoch
Initial learn rate	0.01	Validation frequency	20
Learning rate drop factor	0.5	Minibatch size	128
Learning rate drop period	10	MaxEpochs	30
Learn rate schedule	Piecewise	L2 regularisation	0.0001

NETWORK PERFORMANCE

Validation was carried out in Matlab, and a CNN model was used with a single CPU. The proposed CNN model was evaluated using the hybrid ship inverter fault data and the optimisation algorithm described in the previous section. Fault diagnosis is usually the main consideration when evaluating the accuracy performance of a diagnostic system. Fig. 6 shows the results for the training process of the network. After roughly 80 iterations, i.e. two epochs, the network gradually converges, and the correctness and loss of the model gradually smooths out, giving good results.

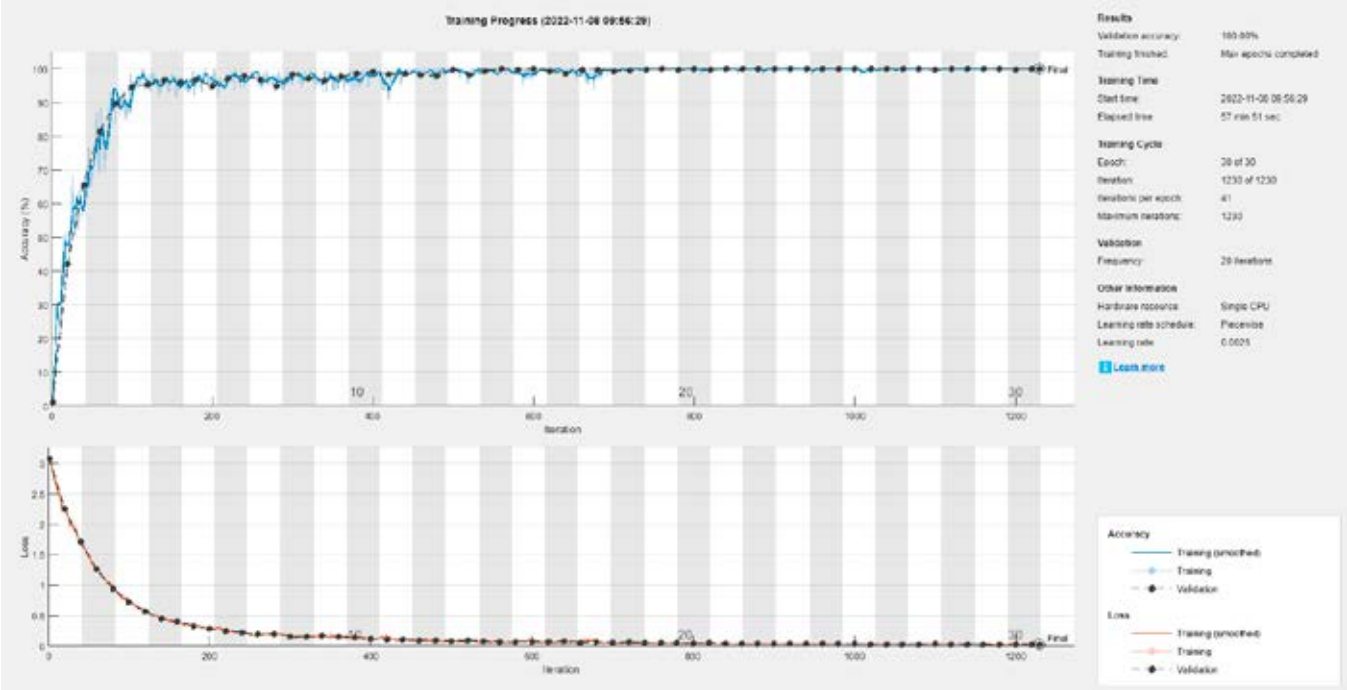

Fig. 6. Training and validation process of the CNN model

The main concern in a CNN model is accuracy. The proposed inverter fault diagnosis model on test data for ten times, which gave an average accuracy of 99.70%, representing very good results.

NOISE TESTS

A real multi-energy hybrid ship has many electrical devices, and the inverter must operate in a harsh environment. The collected signals also contain random interference noise, which affects the effectiveness of fault diagnosis. The signal-to-noise ratio (SNR) is the ratio of the average power of the effective signal to the average power of the noise, and is expressed mathematically as follows:

$$SNR = 10log_{10}\frac{P_{Signal}}{P_{Noise}} \quad (2)$$

where P_{Signal} is the energy of the effective signal, and P_{Noise} is the energy of the noise.

The smaller the SNR, the greater the proportion of noise in the signal. To simulate the noise interference problem in the sampling process, Gaussian white noise was added to the signal with SNRs of 1, 10, 20 and 30dB, to verify the robustness of our CNN fault diagnosis model under several levels of strong noise perturbation. Gaussian white noise is a random variable with a normal probability distribution, with uncorrelated second-order moments and constant first-order moments. The results for the signal of the phase voltage u_a under normal conditions and with the addition of noise with an SNR of 10dB are shown in Fig. 7. Although the voltage signal is very strong, it is still greatly affected by noise, and the signal no longer shows local details but only the overall contour, which makes it difficult to extract effective fault characteristic information.

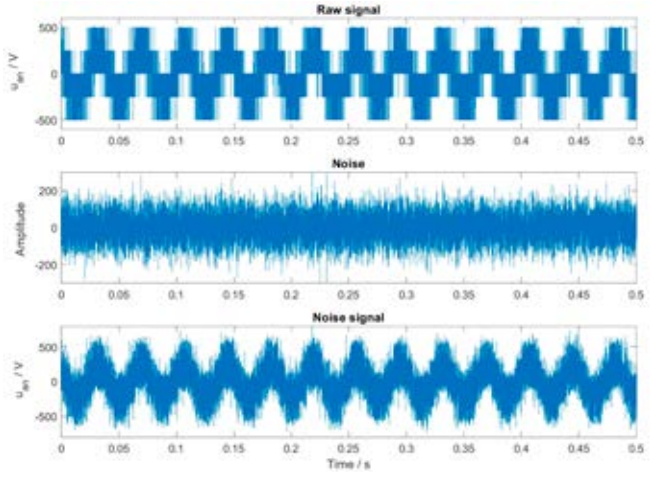

Fig. 7. Composite noise signal with normal inverter and SNR =10dB

The proposed CNN fault diagnosis model was used to process the data in four noisy states, using the same parameters as given above. Five sets of training and testing were performed for each group of noisy cases, and the main results are shown in Table 6 below. It can be seen that even in the presence of noise, our CNN model still gives good results, and the accuracy is above 98% in all cases. At an SNR value of 10dB or above, the accuracy is greater than 99.5%, and the diagnosis results are very good.

Tab. 6. Average parameters for CNN models under four SNRs

SNR(dB)	Average training accuracy (%)	Average verification accuracy (%)	Average test accuracy (%)	Average loss
1	98.35	98.28	98.23	0.076
10	99.33	99.27	99.24	0.053
20	99.43	99.34	99.39	0.040
30	99.62	99.49	99.51	0.032

CONCLUSIONS

This paper presents a one-dimensional CNN-based fault diagnosis model for three-phase voltage source inverters. The proposed model can directly process the original voltage signal without the need for a tedious manual feature extraction process. Experimental results verify that our model can achieve a very high diagnostic accuracy in the pure signal mode, and can also reach an accuracy of over 99.5% under low noise conditions, making it practical for inverter fault diagnosis of a ship's DC electrical system.

ACKNOWLEDGEMENTS

This work was supported by the Science & Technology Commission of Shanghai Municipality and Shanghai Engineering Research Center of Ship Intelligent Maintenance and Energy Efficiency, under Grant 20DZ2252300

DECLARATION OF COMPETING INTEREST

The authors declare that they have no known competing financial interests or personal relationships that could have appeared to influence the work reported in this paper.

REFERENCES

1. Yupeng Yuan, Jixiang Wang, Xinping Yan, Boyang Shen, Teng Long, "A review of multi-energy hybrid power system for ships," *Renewable and Sustainable Energy Reviews*, vol. 132, p. 10081, 2020, https://doi.org/10.1016/j.rser.2020.110081.

2. M. Kunicka and W. Litwin, "Energy efficient small inland passenger shuttle ferry with hybrid propulsion—Concept design, calculations and model tests," *Polish Marit. Res.*, vol. 26, no. 2, 2019, doi: 10.2478/pomr-2019-0028.

3. IEEE Recommended Practice for 1 kV to 35 kV Medium-Voltage DC Power Systems on Ships, *IEEE Std 1709-2018 (Revision of IEEE Std 1709-2010)*, pp. 1-54, 2018, doi: 10.1109/IEEESTD.2018.8569023.

4. N. Bennabi, J. F. Charpentier, H. Menana, J. Y. Billard and P. Genet, "Hybrid propulsion systems for small ships: Context and challenges," *2016 XXII International Conference on Electrical Machines (ICEM)*, 04-07 September 2016, Lausanne, Switzerland, pp. 2948-2954, doi: 10.1109/ICELMACH.2016.7732943.

5. N. Bayati and M. Savaghebi, "Protection systems for DC shipboard microgrids," *Energies*, vol. 14, p. 5319, 2021, https://doi.org/10.3390/en14175319.

6. K. Satpathi, A. Ukil, and J. Pou, "Short-circuit fault management in DC electric ship propulsion system: Protection requirements, review of existing technologies and future research trends," *IEEE Transactions on Transportation Electrification*, vol. 4, no. 1, pp. 272-291, March 2018, doi: 10.1109/TTE.2017.2788199.

7. M. Wu and M. Collier, "Extending the lifetime of heterogeneous sensor networks using a two-level topology," in *2011 IEEE 11th International Conference on Computer and Information Technology*, 31 August 2011 - 02 September 2011, Pafos, pp. 499-504, doi: 10.1109/CIT.2011.64.

8. H. Yang, T. Wang and Y. Tang, "A Hybrid Fault-Tolerant Control Strategy for Three-phase Cascaded Multilevel Inverters Based on Half-bridge Recombination Method," *IECON 2021 – 47th Annual Conference of the IEEE Industrial Electronics Society*,13-16 October 2021, Toronto, ON, Canada,pp. 1-6, doi: 10.1109/IECON48115.2021.9589527.

9. H. -d. Liu, J. -y. Han, N. -j. Shen and H. Lan, "Rectifier Power Thyristor Failure in Real-Time Detection Methods," *2012 Asia-Pacific Power and Energy Engineering Conference*, 27-29 March 2012, Shanghai, China, pp. 1-4, doi: 10.1109/APPEEC.2012.6307672.

10. P. Sobanski and M. Kaminski, "Application of artificial neural networks for transistor open-circuit fault diagnosis in three-phase rectifiers," *IET Power Electronics*, vol. 12, pp. 2189-2200, 2019, https://doi.org/10.1049/iet-pel.2018.5330.

11. M. Yaghoubi, et al., "IGBT open-circuit fault diagnosis in a quasi-Z-source inverter," *IEEE Trans. Ind. Electron.*, vol. 66, no. 4, pp. 2847-2856, 2019.

12. J. K. Nøland, F. Evestedt, and U. Lundin, "Failure modes demonstration and redundant postfault operation of rotating thyristor rectifiers on brushless dual-star exciters," *IEEE Transactions on Industrial Electronics*, vol. 66, no. 2, pp. 842-851, Feb. 2019, doi: 10.1109/TIE.2018.2833044.

13. J. Lamb and B. Mirafzal, "Open-circuit IGBT fault detection and location isolation for cascaded multilevel converters," *IEEE Transactions on Industrial Electronics*, vol. 64, no. 6, pp. 4846-4856, June 2017, doi: 10.1109/TIE.2017.2674629.

14. J. A. Reyes-Malanche, F. J. Villalobos-Pina, E. Cabal-Yepez, R. Alvarez-Salas, and C. Rodriguez-Donate, "Open-circuit fault diagnosis in power inverters through currents analysis

in time domain," *IEEE Trans. Instrum. Meas.*, vol. 70, p. 3517512, 2021.

15. G. Yan, Y. Hu, and J. Jiang, "A novel fault diagnosis method for marine blower with vibration signals," *Polish Maritime Research*, vol. 29, no. 2, pp. 77-86, 2022, https://doi.org/10.2478/pomr-2022-0019.

16. G. Jin, T. Wang, Y. Amirat, Z. Zhou, and T. Xie, "A layering linear discriminant analysis-based fault diagnosis method for grid-connected inverter," *Journal of Marine Science and Engineering*, vol. 10, no. 7, p. 939, 2022, https://doi.org/10.3390/jmse10070939.

17. S. Zhang, R. Wang, Y. Si, and L. Wang, "An improved convolutional neural network for three-phase inverter fault diagnosis," *IEEE Transactions on Instrumentation and Measurement*, vol. 71, pp. 1-15, 2022, art. no. 3510915, doi: 10.1109/TIM.2021.3129198.

18. M. Fahad, M. Alsultan, S. Ahmad, A. Sarwar, M. Tariq, and I. A. Khan, "Reliability analysis and fault-tolerant operation in a multilevel inverter for industrial application," *Electronics*, vol. 11, no. 1, p. 98, 2022, https://doi.org/10.3390/electronics11010098.

19. W. Gong, H. Chen, Z. Zhang, M. Zhang, and H. Gao, "A data-driven-based fault diagnosis approach for electrical power DC-DC inverter by using modified convolutional neural network with global average pooling and 2-D feature image," *IEEE Access*, vol. 8, pp. 73677-73697, 2020, doi: 10.1109/ACCESS.2020.2988323.

20. H. Long, M. Ma, W. Guo, F. Li and X. Zhang, "Fault Diagnosis for IGBTs Open-Circuit Faults in Photovoltaic Grid-Connected Inverters Based on Statistical Analysis and Machine Learning," *2020 IEEE 1st China International Youth Conference on Electrical Engineering (CIYCEE)*, 01-04 November 2020, Wuhan, China ,pp. 1-6, doi: 10.1109/CIYCEE49808.2020.9332538.

21. D. Xie and X. Ge, "A Simple Diagnosis Approach for Multiple IGBT Faults in Cascaded H-Bridge Multilevel Converters," *2020 IEEE Energy Conversion Congress and Exposition (ECCE)*, 11-15 October 2020, Detroit, MI, USA,pp. 5283-5288, doi: 10.1109/ECCE44975.2020.9235463.

22. P. Geng, X. Xu, and T. Tarasiuk, "State of charge estimation method for lithium-ion batteries in all-electric ships based on LSTM neural network," *Polish Marit. Res.*, vol. 27, no. 3, 2020, doi: 10.2478/pomr-2020-0051.

23. T. Wang, H. Xu, J. Han, E. Elbouchikhi, and M. E. H. Benbouzid, "Cascaded H-bridge multilevel inverter system fault diagnosis using a PCA and multiclass relevance vector machine approach," *IEEE Transactions on Power Electronics*, vol. 30, no. 12, pp. 7006-7018, Dec. 2015, doi: 10.1109/TPEL.2015.2393373.

24. J. Jiao, M. Zhao, J. Lin, and K. Liang, "A comprehensive review on convolutional neural network in machine fault diagnosis," *Neurocomputing*, vol. 417, pp. 36-63, 2020, https://doi.org/10.1016/j.neucom.2020.07.088.

25. Y. Wang, C. Bai, X. Qian, W. Liu, C. Zhu, and L. Ge, "A DC series arc fault detection method based on a lightweight convolutional neural network used in photovoltaic system," *Energies*, vol. 15, no. 8, pp. 2877, 2022, https://doi.org/10.3390/en15082877.

26. X. Wang, B. Yang, Z. Wang, Q. Liu, C. Chen, and X. Guan, "A compressed sensing and CNN-based method for fault diagnosis of photovoltaic inverters in edge computing scenarios," *IET Renew. Power Gener.*, vol. 16, pp. 1434-1444, 2022, https://doi.org/10.1049/rpg2.12383.

27. U. Choi, J. Lee, F. Blaabjerg, and K. Lee, "Open-circuit fault diagnosis and fault-tolerant control for a grid-connected NPC inverter," *IEEE Transactions on Power Electronics*, vol. 31, no. 10, pp. 7234-7247, Oct. 2016, doi: 10.1109/TPEL.2015.2510224.

28. M. Kumar, "Open circuit fault detection and switch identification for LS-PWM H-bridge inverter," *IEEE Transactions on Circuits and Systems II: Express Briefs*, vol. 68, no. 4, pp. 1363-1367, April 2021, doi: 10.1109/TCSII.2020.3035241.

29. K.-H. Chao and Y.-R. Shen, "Application of an extension neural network method for fault diagnosis of three-level inverters used in marine vessels," Journal of Marine Science and Technology, vol. 24, no. 5, Article 8, 2022, doi:10.6119/JMST-016-0604-1.

CONTACT WITH THE AUTHORS

Guohua Yan

Yihuai Hu*
e-mail: yhhu@shmtu.edu.cn

Qingguo Shi

Merchant Marine College
Shanghai Maritime University
China